Journal of Crohn's and Colitis, 2022, **16**, 978–991
https://doi.org/10.1093/ecco-jcc/jjab222
Advance access publication 10 December 2021
Original Article

Selective Targeting of Tumour Necrosis Factor Receptor 1 Induces Stable Protection from Crohn's-Like Ileitis in TNF$^{\Delta ARE}$ Mice

Rajrupa Chakraborty,[a] Mia R. Maltz,[a,b,c] Diana Del Castillo,[a] Purvi N. Tandel,[a] Nathalie Messih,[a,d] Martha Anguiano,[a,e] David D. Lo[a,b,c]

[a]Division of Biomedical Sciences, School of Medicine, University of California, Riverside School of Medicine, Riverside, CA, USA
[b]BREATHE Center, University of California, Riverside, Riverside, CA, USA
[c]Center for Health Disparities Research, University of California, Riverside, Riverside, CA, USA
[d]Department of Evolution, Ecology and Organismal Biology, College of Natural and Agricultural Sciences, University of California, Riverside, Riverside, CA, USA
[e]Department of Chemical and Environmental Engineering, College of Engineering, University of California, Riverside, Riverside, CA, USA

Corresponding author: David D. Lo, MD, PhD, Biomedical Sciences, UCR School of Medicine, 900, University Ave., Riverside, CA 92521, USA. Tel: 951-827-4553; Email: david.lo@medsch.ucr.edu

Abstract

Background and Aims: Crohn's disease is a debilitating chronic inflammatory disorder of the mammalian gastrointestinal tract. Current interventions using anti-tumour necrosis factor [anti-TNF] biologics show long-term benefit in only half of patients. This study focused on the role of the TNF receptor 1 [TNFR1] in pathogenesis in a TNF-driven model of ileitis.

Methods: We studied TNF$^{\Delta AU\text{-rich element [ARE]}/+}$ [TNFdARE] mice, which develop progressive ileitis similar to Crohn's ileitis. Histopathological analysis and gene expression profiling were used to characterize disease progression from 5 to 16 weeks. Mice with TNFR1 hemizygosity [TNFdARE/R1het] allowed us to assess gene dosage effects. Transcriptional profiling established inflection points in disease progression; inflammatory gene expression increased at 8 weeks with a plateau by 10 weeks, so these were selected as endpoints of treatment using the TNF biologic infliximab and the TNFR1-specific XPro1595. Differences in recruitment of cells in the lamina propria were assessed using flow cytometry.

Results: TNFdARE/R1het mice displayed stable long-term protection from disease, associated with decreased recruitment of CD11b^{hi}F4/80^{lo} monocytes and CD11b^{hi}Ly6G^{hi} neutrophils, suggesting an important role of TNFR1 signalling in pathogenesis, and indicating potential benefit from TNFR1-specific intervention. Treatment with infliximab and XPro1595 both showed a similar impact on disease in TNFdARE mice. Importantly, these beneficial effects were greatly surpassed by hemizygosity at the TNFR1 locus.

Conclusions: Treatment with either infliximab or XPro1595 produced moderate protection from ileitis in TNFdARE mice. However, hemizygosity at the TNFR1 locus in TNFdARE mice showed far better protection, implicating TNFR1 signalling as a key mediator of TNF-driven disease.

Received: July 9, 2021. **Revised:** October 25, 2021. **Accepted:** December 8, 2021

Graphical Abstract

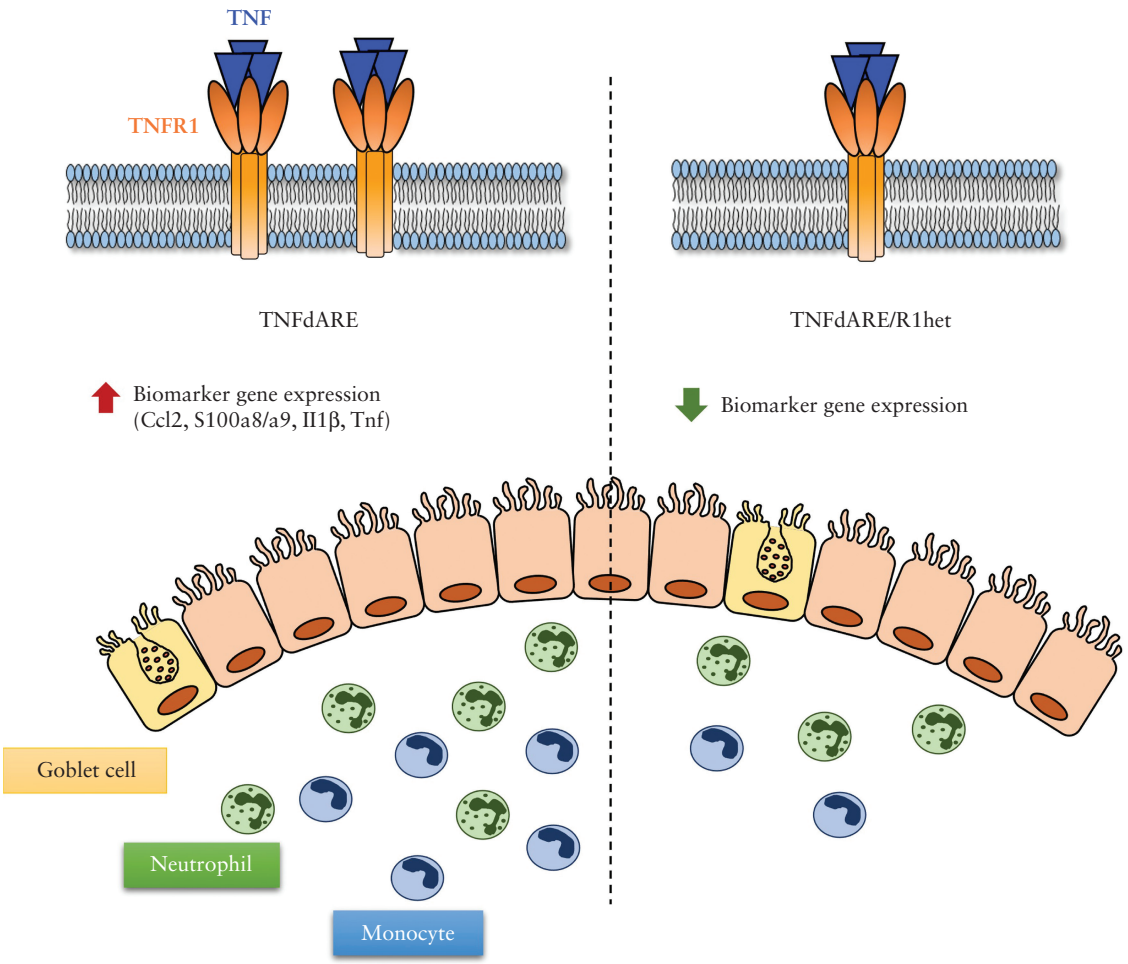

Key Words: TNFdARE; TNFR1; infliximab; XPro1595

1. Introduction

Crohn's disease [CD] is a chronic, relapsing and remitting inflammatory condition of the mammalian gastrointestinal tract that primarily affects the small intestine, specifically the terminal ileum. Although clinical features of this disease vary broadly depending on the disease phenotypes, it is commonly diagnosed with chronic diarrhoea, abdominal pain, fever and weight loss.[1,2] Attempts to identify factors driving this disease have led to the discovery of several susceptibility genes and a better understanding of the involvement of dysregulated immune responses in the disease pathogenesis. Studies using preclinical mouse models of CD have revealed the influence of diet, metabolism and intestinal microbiota and illustrated the contributions of genetics and proinflammatory cytokines in the development of CD.[3–5] Elevated mucosal levels of tumour necrosis factor [TNF]α has been associated with the aetiology of this disease[6,7] and thus, over the years, various therapeutic agents have been designed to target this proinflammatory cytokine.

TNFα is a pleotropic cytokine, which regulates pathways involving intestinal mucosal homeostasis as well as inflammation. TNF interacts with two transmembrane receptors, TNF receptor 1 [TNFR1] and TNFR2, to exert a broad spectrum of biological functions transcending immune system regulation and neuropathology.[8,9] Both soluble and membrane-bound forms of TNF bind to both the receptors, but soluble TNF primarily activates TNFR1[10] whereas membrane-bound TNF is a more potent ligand for TNFR2.[11] TNFR1 is ubiquitously expressed in the host and predominantly mediates pro-inflammatory and pro-apoptotic signalling pathways; TNFR2, by contrast, is primarily expressed on haematopoietic and endothelial cells and exerts neuroprotective functions and also promotes tissue regeneration and homeostasis.[12–14]

Treatment with anti-TNF antibodies has been an integral part of IBD therapy for the last two decades but existing therapeutics are not universally effective. About 30% of patients respond to anti-TNF therapy but almost 50% lose clinical benefits within the first year of their treatment.[15] While it is an ongoing challenge to understand the underlying mechanisms of clinical non-response in patients, it is also crucial to develop broadly effective therapeutic approaches.

In the present work, we characterized the role of TNFR1 in the pathogenesis of CD using TNFdARE mice, which harbour a mutation in a regulatory element in the TNFα transcript resulting in over-production of TNFα; these mice exhibit many features similar to Crohn's ileitis in humans.[16] To this end, we have developed a method based on the transcriptional expression of a distinct set of genes that correlate with the trajectory of progressive ileitis in these mice. Using infliximab and a TNFR1-specific inhibitor [XPro1595] in a controlled drug

intervention study, we show that these therapeutic agents produced a similar degree of protection in TNFdARE mice. Interestingly, protective effects were more robust and stable in TNFdARE/R1het mice, which underlines the potential benefits of selective targeting of TNFR1 over global TNF blockade in the treatment of CD.

2. Materials and Methods

2.1. Animals

Animal studies were performed using IACUC-approved protocols and following guidelines from University of California, Riverside [UCR] and the National Institutes of Health [NIH]. TNFdARE mice were obtained from Dr Fabio Cominelli at the Case Western Reserve University to establish a breeding colony and TNFdARE/R1het mice were generated by backcrossing with TNFR1$^{-/-}$ mice [Jax strain #003242; Jackson laboratory] maintained in a C57BL/6 background in our vivarium. TNFdARE mice were backcrossed to peptidoglycan recognition protein-S [PGRP-S]-dsRed transgenic mice[17] to generate TNFdARE/PGRP-S-dsRed [dsRed+TNFdARE] mice. TNFdARE/occludin-eGFP double transgenic mice were generated by backcrossing dsRed+TNFdARE/R1het mice with villin-eGFP-occludin transgenic mice [obtained from Dr Jarrold R. Turner at the Brigham and Women's Hospital and Harvard Medical School] where expression of the occludin-eGFP fusion reporter transgene was regulated by the villin promoter.[18] Some TNFdARE mice used in this study had mixed genetic backgrounds as they were generated by backcrossing TNFdARE mice on a C57BL/6J background with PGRP-S-dsRed mice that had been maintained on a mixed background with suspected BALB/c contamination of unknown amount. In separate studies, TNFdARE mice were backcrossed with BALB/cJ mice [Jax strain #000651; Jackson laboratory] so that F1 generation mice could be compared with the TNFdARE mice harbouring suspected mixed backgrounds. Mice were maintained in a conventional specific pathogen-free facility at UCR and provided food and inhouse RO water *ad libitum*.

TNFdARE mice [8 weeks old] were intraperitoneally administered with either BSA [10 mg/kg; Invitrogen] or XPro1595 [10 mg/kg; INmuneBio Inc.] and either Isotype control [human $IgG_{1\kappa}$; 100 µg per mouse; Southern Biotech] or infliximab [100 µg per mouse; Pfizer Inc.] twice a week for 15 days before being killed at 10 weeks to determine benefits from therapeutic drugs. Mice were anaesthetized with isoflurane [Covetrus] and killed by cervical dislocation. Approximately 1 cm of the distal ileum was dissected and stored in 1 ml RNAlater [Invitrogen] at −80°C for RNA extraction. Then, 2–2.5 cm of the remaining distal ileum was cut into ~1-mm pieces, half of which were embedded in OCT, snap frozen in liquid nitrogen and stored at −80°C for cryosectioning. The remaining tissue pieces were fixed in 10% neutral buffered formalin [NBF] at 4°C for 24 h, which were then washed twice with chilled 1× phosphate buffered saline [PBS] and then stored in 70% ethanol at 4°C until further processing.

2.2. RNA extraction

Tissues were removed from RNAlater and ~10–15 mg was used to extract RNA using an RNeasy kit (Qiagen) following the manufacturer's instructions. Genomic DNA was digested using DNase Max kit [Qiagen] and RNA was eluted in RNase-free water. The concentration of RNA was measured using a NanoDrop 2000 [Thermo Scientific].

2.3. Gene expression analysis

Extracted RNA was diluted in RNase-free water and 50 ng was run on an nCounter Sprint Profiler [Nanostring Technologies] using the nCounter Mouse Immunology Panel following the manufacturer's instructions. Transcriptional expression of a total of 561 genes was assessed using the nSolver 4.0 software and false discovery rates were calculated by the Benjamini–Hochberg method. Normalized data were used to calculate fold changes in gene expression unless otherwise stated.

Differences in intestinal immune gene expression profiles [from the nCounter Mouse Immunology Panel] for each mouse sampled were analysed using principal component analyses [PCAs][19] using the DEseq2 package in R version 4.0.3 [R version 4.0.3; R Core Team 2020]. We used regularized log transformation to transform the gene expression data, using the *rlog* function. Matrices were constructed as data points projected onto the 2-D plane, such that the variance is maximized. As dimensions were reduced, they spread out in two directions to explain most of the differences in the data. The *x*-axes [labelled as PC1] in the ordination space represent the first principal component, which separates data points to represent the most variation in the dataset; *y*-axes [labelled as PC2] are orthogonal to PC1 and separate data points to represent the next greatest amount of variation within these gene expression datasets, across mouse genotypes or ages. We used the function *plotPCA* to visualize these PCA plots in R [R version 3.2.1; R Core Team 2017]. We conducted differential gene expression analyses with the data object *dds* as the input for the function *DESeq*. *DESeq2* performs a hypothesis test for each gene to see whether the observed data provide enough evidence for confirming significant differences in differentially expressed genes across experimental conditions. The *p*-values were adjusted to control for multiple comparisons using the Benjamini–Hochberg method. We compared the probability that a *log2FoldChange* in gene expression would change due to one group, as compared to another sample group. Normalized raw data tables mentioned in the text [Supplementary Tables] have been posted to Dryad: [doi:10.5061/dryad.8cz8w9gr4].

2.4. Histology

Distal ileal tissues fixed in 10% NBF were processed in an automated processor, paraffin-embedded and sectioned at 5-µm thickness for haematoxylin and eosin [H&E] staining. Images were acquired using Keyence BX-X710 [Keyence Corp.]. Image composites were generated using Adobe Photoshop 22.4.2 and scored for accumulation of immune cells in the villi and alterations in villous architecture on a scale of 1 to 4; 1 = healthy villi; 2 [mild disease] = ≤50% of the total number of villi counted had infiltrates with incidence of villous blunting; 3 [moderate disease] = >50% but <75% of villi had infiltrates with higher incidence of villous blunting, villous clubbing may be visible; and 4 [severe disease] = >75% of villi had infiltrates with severe villous blunting and increased presence of clubbed-shaped villi.

Formalin [10% NBF]-fixed paraffin-embedded tissues were used for Alcian Blue staining to identify goblet cells. After deparaffinization and hydration, tissues were stained with Alcian Blue reagent for 30 min. Then, tissues were washed and counterstained with nuclear Fast Red for 5 min. Before

mounting, tissues were washed, dehydrated and cleared in xylene. Mucus-containing goblet cells were enumerated in 20 villi per sample and an average was calculated to determine the number of mucus-containing goblet cells per villus.

For immunostaining, frozen tissues were sectioned at 15-µm thickness in a cryostat and fixed in 4% paraformaldehyde [PFA[before permeabilization with 0.5% Tween-20/1× PBS followed by blocking in 0.1% Tween-20/1× PBS containing 5% normal goat serum. Tissue sections were stained with an antibody against B220 conjugated with fluorescein isothiocyanate [FITC; eBioscience] or Alexa Fluor 488 [eBioscience], and DAPI [Invitrogen] was used to stain nuclei. Images were acquired using a spinning-disc confocal microscope [Zeiss] and analysed using ImageJ software and Adobe Photoshop 22.4.2.

2.5. Isolation of immune cells from small intestinal lamina propria

Small intestines were dissected from mice and cut longitudinally to remove faecal material by washing in chilled 1× PBS. Tissues were cut into ~5-mm pieces and treated with HBSS medium supplemented with 5% fetal bovine serum [FBS], 1 mM DTT and 2 mM EDTA to remove mucus and loosen cell junctions. Next, tissues were incubated in a solution containing HBSS medium supplemented with 5% FBS and 2 mM EDTA to strip epithelial cell lining followed by digestion in RPMI supplemented with 5% FBS, collagenase D [Roche] and DNase I [Worthington]. Digested tissues were mechanically dissociated with a 3-mL syringe plunger and lamina propria cells were washed with DMEM [with a high concentration of glucose] supplemented with 5% FBS while filtering successively through 100- and 40-µm cell strainers. Cells were pelleted by centrifuging at 2000 r.p.m. for 5 min at 4°C and then stained.

2.6. Flow cytometry

Small intestinal lamina propria cells were resuspended in a 1:50 dilution of F_C block [BD Pharmingen; Clone 2.4G2] in FACS buffer containing 5 mM EDTA and incubated on ice for 10 min. Cells were then stained with fluorophore-conjugated primary antibodies for 30 min on ice before fixing with 2% PFA: anti-CD45 FITC [BioLegend; clone 30-F11], anti-CD19 APC [BD; clone 1D3], anti-CD3 Alexa Fluor 700 [BioLegend; clone 17A2], anti-Ly6G BV510 [BioLegend; clone 1A8], anti-F4/80 PE [BioLegend; clone BM8] and anti-CD11b BV421 [BioLegend; clone M1/70]. Splenocytes were used for single colour controls. Samples were run on a NovoCyte Advanteon Flow Cytometer system [Agilent] and data analysis was performed using FlowJo [version 10.7.1].

2.7. Statistical analysis

All data presented are shown as mean ± SD unless otherwise mentioned. Statistical analysis was performed using Prism software 9.1.2 [GraphPad]. Statistical significance was calculated by either Student's *t*-test with Welch's correction or non-parametric Mann–Whitney U test.

3. Results

3.1. Characterization of progressive ileitis in TNFdARE mice

In this study, we used TNFdARE mice to investigate the role of TNFR1 in progressive ileitis and to compare the benefits of global TNFα blockade vs selective modulation of TNFR1. We used transcriptional profiling of immune-related genes as a primary method to characterize disease progression in 5- to 16-week-old TNFdARE mice. Figure 1A shows relative quantification of an array of genes, which were upregulated in TNFdARE mice in comparison to wild-type [WT] littermate controls. These genes showed unique expression trajectories accompanied by either a gradual or sharp upregulation starting from 8 weeks that plateaued after 10 weeks except S100a8 and S100a9, which continued to increase over time. Based on these differential patterns of expression, subsets of genes were categorized into four clusters; 'Cluster 1' encompassed S100a8 and S100a9 that showed high induction early around 6 weeks, followed by a slight decline and then a steady increase; 'Cluster 2' only had Ccl2 that showed early high expression followed by a slow and shallow upregulation up to 16 weeks; C3 and Il1b were included in 'Cluster 3', which showed steady upregulation from 5 to 10 weeks, reaching a plateau thereafter; and 'Cluster 4' included a group of genes that showed sharp upregulation starting no sooner than around 8 weeks and reaching a plateau at 10 weeks, stabilizing in expression thereafter. These findings point to a main inflection point in disease progression at around 8 weeks associated with abrupt upregulation in expression of proinflammatory genes that, for many genes, stabilized at a plateau after 10 weeks. Based on this gene expression profile, we selected 8 and 10 weeks as the start and endpoints, respectively, as a susceptible period to evaluate drug therapeutic effects.

Fold changes in expression of genes in the immunology panel are given in Supplementary Table 1. Some mice used in these experiments had suspected mixed genetic backgrounds. We compared expression of selected proinflammatory genes from the gene clusters described above in 10- to 11-week-old inhouse TNFdARE mice harbouring suspected mixed [C57BL/6;BALB/c] genetic backgrounds and TNFdARE mice heterozygous for BALB/c genetic background to determine differences in disease activity. We observed no significant differences in fold changes of proinflammatory gene expression [Supplementary Figure 1], suggesting no significant impact of mouse genetic background on progressive ileitis in TNFdARE mice. A normalized dataset with fold changes in gene expression in TNFdARE-BALB/c F1 mice is included in Supplementary Table 2.

Using PCA, we illustrate the trajectory of disease progression of TNFdARE mice from 5 to 16 weeks of age, along with comparisons to WT littermates [Figure 1B]. At early time points, 5- and some 7-week-old TNFdARE mice clustered closer to their WT littermates, showing that the gene expression profiles of these mice were, to some extent, comparable without clear evidence of disease. As mice got older, gene expression changes representative of progressive ileitis drove segregation of the TNFdARE mice further away from younger mice as well as WT littermates. Moreover, among the oldest TNFdARE mice, individual differences further increased, with greater scatter of these data points. Interestingly, 16-week-old TNFdARE mice were clustered together, suggesting a stable end-stage of disease. We did not observe any noticeable influence of gender on ileitis progression in TNFdARE mice [data not shown].

To quantitatively assess the severity of disease pathogenesis in TNFdARE mice, we performed histopathological scoring on H&E-stained intestinal tissue sections from mice of different

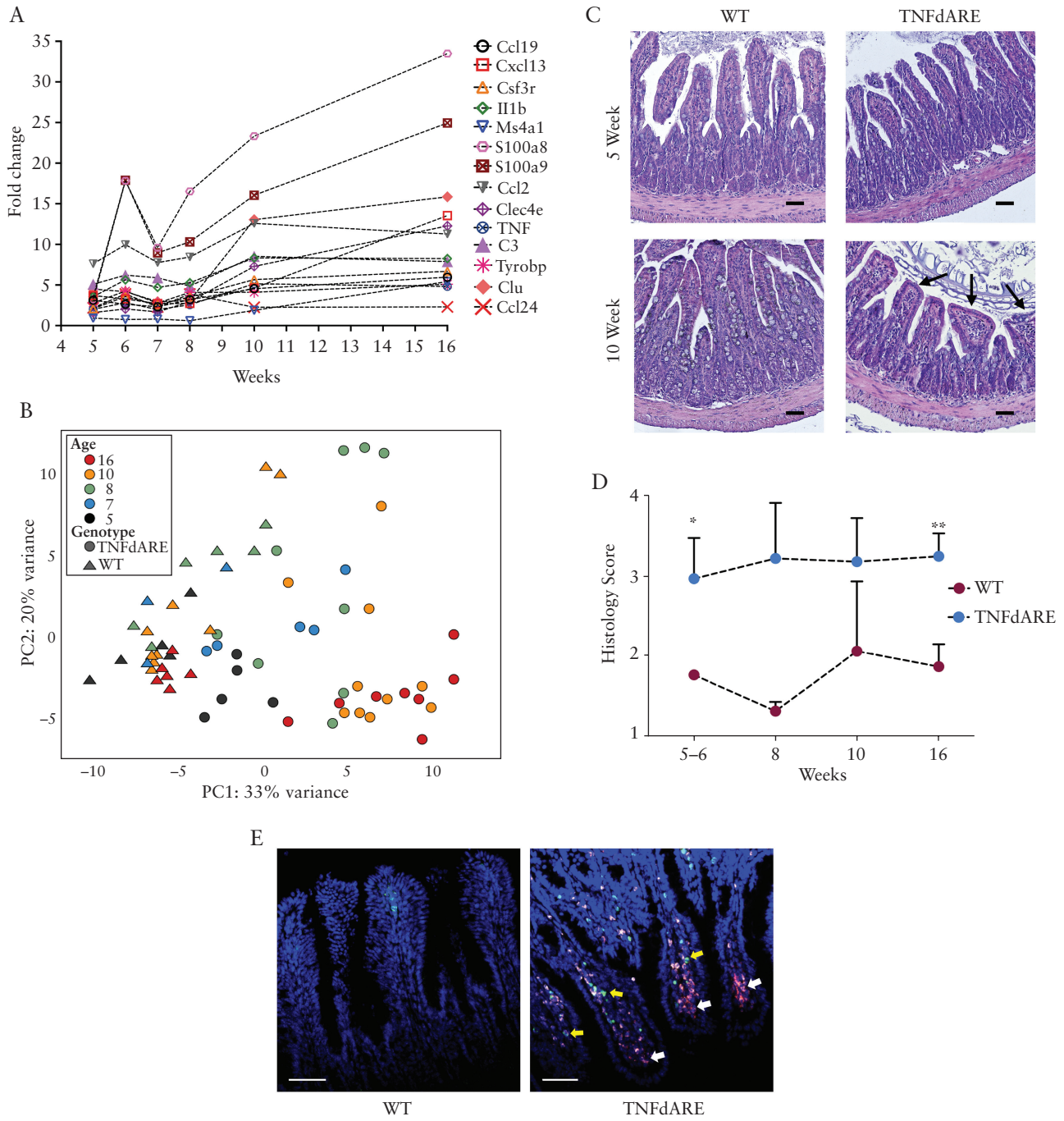

Figure 1. Characterization of ileitis progression in TNFdARE mice. [A] Kinetics of differential expression of gene clusters in 5- to 16-week-old TNFdARE mice. Data were normalized to WT littermate controls at each time point. [B] PCA plot showing the spatial distribution of 5- to 16-week-old TNFdARE mice and WT littermates across a two-dimensional plot; n = 3–9 mice per genotype. [C] H&E staining on paraffin-embedded terminal ileal tissue sections obtained from 5- and 10-week-old TNFdARE mice and WT littermates. Villi blunting in 10-week-old TNFdARE mice indicated in black arrows; scale bar = 50 μm. [D] H&E-stained ileal tissue sections from WT and TNFdARE mice were scored for villous aggregates of immune cells, surface epithelial integrity and villous blunting [n = 3–7 mice per genotype]. [E] B cell staining [yellow arrows] with αB220 [FITC] antibody on ileal cryosections obtained from 10-week-old PGRP-S-dsRed+ WT and TNFdARE mice showing neutrophil [dsRed+] accumulation [white arrows] in the villi. Nuclei stained with DAPI. Scale bar = 50um; n = 3–5 mice per group. *, $p < 0.05$; **, $p < 0.01$ calculated by Student's t-test with Welch's correction.

ages [Figure 1C and D]. The scoring strategy was primarily based on two criteria: accumulation of immune cells in the lamina propria and increased incidence of villous clubbing, defined here as accumulation of infiltrating immune cells near the tip of the villi, with narrowing of the villi below the accumulated infiltrates. Increased accumulation of immune cells was observed in the lamina propria of both younger [5–6 weeks old] and older [8, 10 and 16 weeks old] TNFdARE mice compared to that in WT littermates, suggesting an early recruitment of proinflammatory cells that may drive disease progression in these mice. Interestingly, villous clubbing appeared to be more extensive in the older TNFdARE mice, which was also accompanied by an increased incidence of villous blunting, here defined as a flattening of the villous tip

due to accumulated infiltrates [Figure 1C, lower panel to the right], previously identified as a distinct feature of progressive ileitis in TNFdARE mice.[16] Additionally, we performed immunostaining on ileal cryosections obtained from 10-week-old dsRed+ WT and TNFdARE mice to ascertain infiltration of neutrophils and B cells in the villi. Unlike WT littermates, dsRed+ TNFdARE mice exhibited increased accumulation of neutrophils and B cells in the villi, suggesting marked acute and chronic inflammation consistent with progression of ileitis [Figure 1E].

3.2. Stable protection from ileitis in TNFdARE/R1het mice

Our preliminary observations suggested that TNFdARE/R1het mice were, to some extent, protected from severe ileitis. We decided to focus on TNFdARE/R1het and not TNFdARE/R1 knockout mice in this study because TNFdARE/R1 knockout mice have been described previously[16,20] and because TNFR1 hemizygosity may more closely physiologically resemble the effects of TNFR1-targeted therapeutics than a homozygous knockout system as therapeutic strategies rarely achieve complete blockade of any receptor signalling system *in vivo*.

To characterize the protective effects in TNFdARE/R1het mice, we first compared gene expression profiles of TNFdARE and TNFdARE/R1het mice and focused on selected proinflammatory genes from the gene clusters described in Figure 1A. Quantification of these genes revealed distinct suppression of progressive ileitis in 8-week-old TNFdARE/R1het mice, which became more pronounced at 10 and 16 weeks [Figure 2A–C]. This was supported by PCA showing a clear distinction in the overall gene expression phenotypes of TNFdARE and TNFdARE/R1het mice at 16 weeks of age [Figure 2D]. Normalized datasets with fold changes in expression of genes in the immunology panel are shown in Supplementary Table 1. Interestingly, histological analysis of intestinal tissues from 8-, 10- and 16-week-old TNFdARE and TNFdARE/R1het mice showed almost overlapping degrees of immune cell accumulation in the villi, and villous clubbing was also noticed, although to a lesser extent, in the latter [Figure 2E and F] suggesting no significant contribution of TNFR1 hemizygosity on histological benefits at least up to 16 weeks of age. Overall, these results reveal that TNFdARE/R1het mice developed a stable, low-grade ileitis phenotype in contrast to the progressive severe disease in TNFdARE mice, suggesting a critical role of TNFR1 signalling in disease pathogenesis. We enumerated goblet cells in 10-week-old WT, TNFdARE and TNFdARE/R1het mice to investigate the effect of chronic inflammation or TNFR1 hemizygosity respectively on goblet cell differentiation. We observed significantly increased numbers of mucus-containing goblet cells in both TNFdARE and TNFdARE/R1het mice compared to that in WT littermates despite an apparent protective effect of TNFR1 hemizygosity [Figure 2G and H]. The similar level of induction in both TNFdARE and TNFdARE/R1het mice suggests that induction of goblet cells requires only minimal chronic inflammation.

3.3. TNFR1-specific blockade suppresses active progression of ileitis in TNFdARE mice

Based on the evidence presented in Figure 2, we hypothesized that selective targeting of TNFR1 could provide protective benefits against ileitis. For these studies, we tested XPro1595 to investigate beneficial effects in TNFdARE mice. XPro1595 is a second-generation TNF inhibitor that selectively interacts with soluble, but not membrane-bound, TNF, thereby forming a heterotrimer and sequestering soluble TNF from binding to TNFR1[21–24] without altering signalling through TNFR2. XPro1595 [10 mg/kg] or BSA [control] was administered intraperitoneally to 8-week-old TNFdARE mice, as this was determined as the inflection point in disease progression [Figure 1A], and after 2 weeks beneficial effects were studied by transcriptional profiling and histological analysis. Using relative quantification of the same set of proinflammatory genes described in Figure 1A as disease biomarkers, we showed that TNFdARE mice treated with XPro1595 exhibited a significant reduction in disease activity compared to the BSA-treated controls or treatment-naïve TNFdARE mice [Figure 3A]. However, the magnitude of suppression, although significant, was still not as pronounced as the effect seen in TNFdARE/R1het mice. Supplementary Table 3 shows normalized datasets with fold changes in expression of genes used for transcriptional profiling. Additionally, histological grading of TNFdARE mice treated with BSA or XPro1595 showed a marked decline in disease activity in many of the drug-treated mice, which therefore qualified for a low histological score, compared to those treated with BSA, but this difference was not statistically significant [Figure 3B]. We also noted a high accumulation of neutrophils and B cells in the villi of TNFdARE mice treated with BSA, which was substantially reduced in mice treated with XPro1595 [Figure 3C]. No statistical significance was observed when goblet cell counts were compared between TNFdARE mice treated with either BSA or XPro1595 [Supplementary Figure 2], suggesting no effect of XPro1595 on goblet cell differentiation in TNFdARE mice.

3.4. Global TNF blockade mitigates ileitis in TNFdARE mice

Infliximab was the first FDA-approved anti-TNF therapeutic agent that showed promising clinical responses in treating IBD[-].[25–28] We included infliximab in our drug intervention studies as a reference to quantitatively assess the protective benefits of XPro1595 in TNFdARE mice. Infliximab [100 µg] or an isotype control antibody was intraperitoneally administered to 8-week-old TNFdARE mice for 2 weeks before examining the beneficial effects by gene expression and histological analysis. Pairwise comparisons between the treatment groups, using relative quantification of disease biomarker genes, showed significant suppression of biomarker gene expression in infliximab-treated mice compared to isotype controls or treatment naïve TNFdARE mice [Figure 4A]. Despite this effect, however, it was not as potent as the effect seen in TNFdARE/R1het mice. Supplementary Table 3 shows normalized datasets with fold changes in expression of genes used for transcriptional profiling. As with XPro1595 treatment, histological scores showed improvement in some individual mice treated with infliximab but not enough to show significant benefit among the whole treated group [Figure 4B]. Immunostaining of cryosections from TNFdARE mice treated with either infliximab or an isotype control showed recruitment of neutrophils and B cells in the villi that was comparable between the two groups [Figure 4C], thereby corroborating our results from histopathological scoring of these mice. We did not observe any significant difference in the abundance of goblet cells between TNFdARE mice treated with infliximab

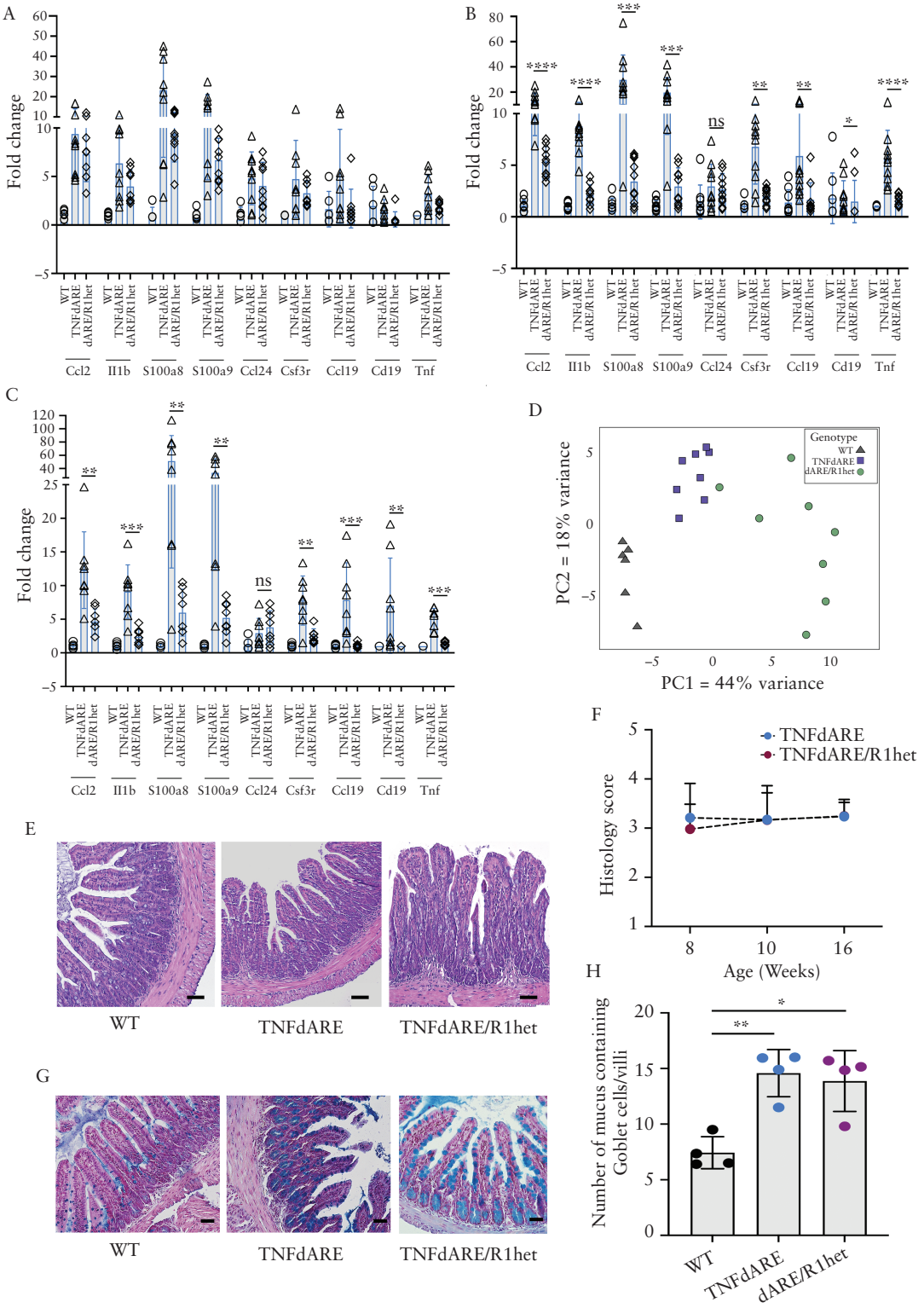

Figure 2. Suppression of ileitis in TNFdARE/R1het mice. Pairwise comparisons of relative expression of biomarker genes signifying active progression of ileitis in 8- [A] 10- [B] and 16-week-old [C] TNFdARE and TNFdARE/R1het mice. Data normalized to gene expression in WT littermates at each time point; n = 6–10 mice per genotype. [D] PCA plot showing the distribution of 16-week-old WT, TNFdARE and TNFdARE/R1het samples in a two-dimensional plot; n = 6–8 mice per genotype. [E] Representative H&E-stained images from terminal ileum of 16-week old WT, TNFdARE and TNFdARE/R1het mice; scale bar = 50 µmm. [F] H&E-stained ileal tissue sections from 8-, 10- and 16-week-old TNFdARE and TNFdARE/R1het mice were scored for immune cell infiltration in the lamina propria, villous blunting and alteration in overall epithelial architecture [n = 3–7 mice per group]. [G] Representative images showing Alcian Blue staining for goblet cells in formalin-fixed, paraffin-embedded ileal tissue sections from 10-week-old WT littermate control, TNFdARE and TNFdARE/R1het mice; scale bar = 50 µm. [H] Mucus-containing goblet cells were enumerated from 20 villi per mouse and the number of goblet cells per villi was represented; n = 4 mice per genotype. *, $p < 0.05$; **, $p < 0.01$;***, $p < 0.001$; ****, $p < 0.0001$ calculated by non-parametric Mann–Whitney U-test. A Student's t-test with Welch's correction was used to calculate statistical significance for goblet cell counts.

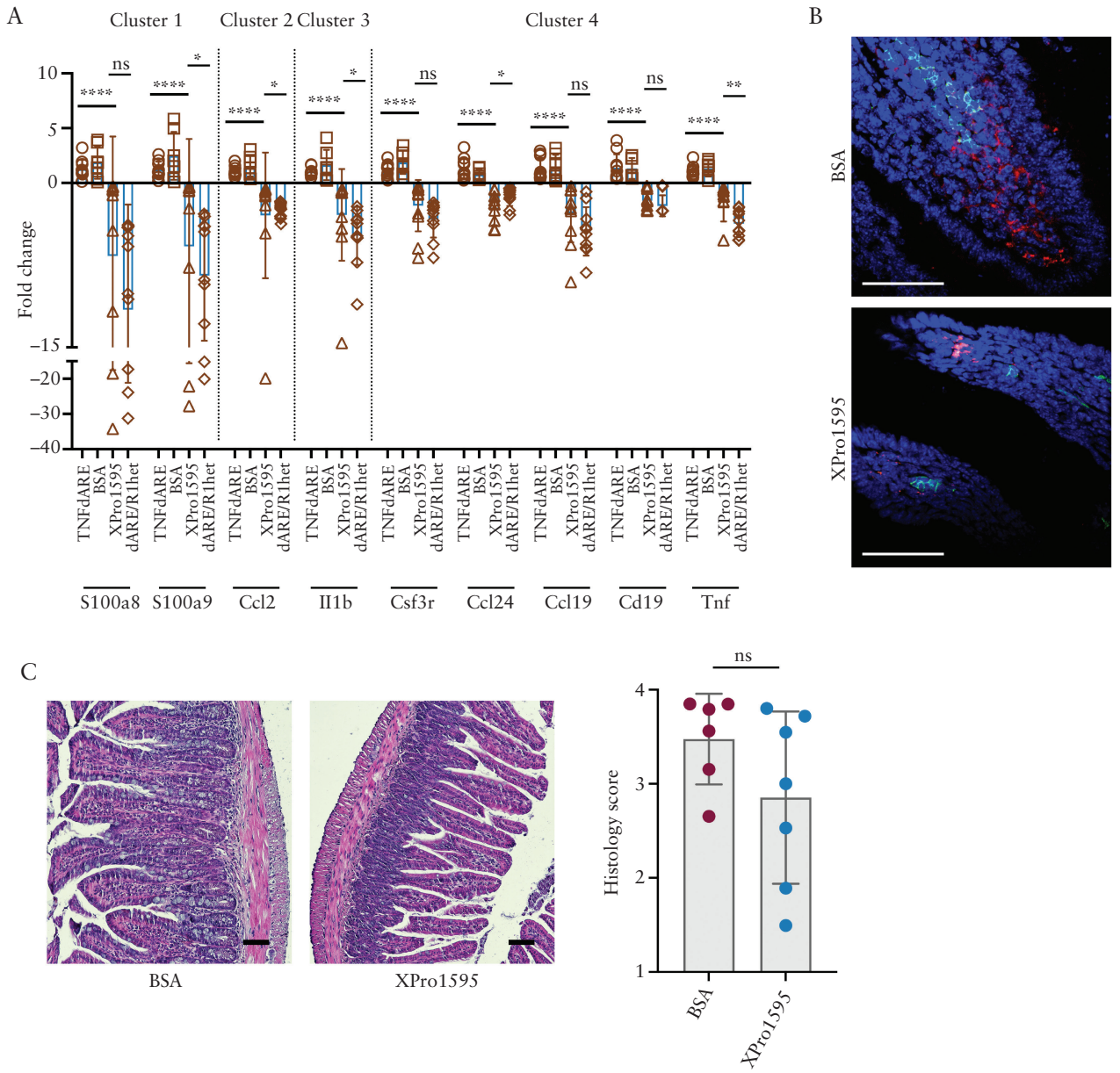

Figure 3. Drug intervention using XPro1595 suppresses active progression of ileitis in TNFdARE mice. [A] Pairwise comparison of relative expression of gene clusters used as signature biomarkers for progression of ileitis in TNFdARE mice. Transcriptional expression was normalized to that of treatment-naive TNFdARE mice and compared between TNFdARE/R1het and TNFdARE mice treated with either BSA [control] or XPro1595; n = 7–11 mice per group. [B] H&E staining on ileal tissue sections from BSA- and Xpro1595-treated TNFdARE mice [left] along with histology scores [right] [n = 6–7 mice per group]. Scale bar = 50 μm. [C] Anti-B220 [Alexa 488] staining on ileal cryosections from PGRP-S-dsRed+ TNFdARE mice treated with either BSA or XPro1595 showing aggregates of B cells [green] and neutrophils [dsRed+] in the villi. Nuclei stained with DAPI. Scale bar = 50 μm [n = 3–4 mice per group]. ns, not significant; *, $p < 0.05$; **, $p < 0.01$; ****, $p < 0.0001$ calculated by non-parametric Mann–Whitney U-test.

or isotype control [Supplementary Figure 3], suggesting no impact of infliximab on goblet cell differentiation.

3.5. TNFdARE/R1het mice show robust protection against ileitis

Our studies treating TNFdARE mice with either infliximab or XPro1595 showed that despite clear protective effects of both treatments, neither treatment was as potent as the impact of TNFR1 gene dosage. The basis of the TNFR1 hemizygosity-mediated protective effect is not clear, but further analysis provided some clues to the role of TNFR1 in both disease progression and protection in TNFdARE/R1het mice. While TNFdARE/R1het mice showed stable long-term protection from progressive disease, they still maintained a persistent low-grade inflammation in the lamina propria [Figure 2E and F], suggesting that the inflammatory response in the ileum had reached a point of steady-state equilibrium.

Further analysis comparing the effects of infliximab and Xpro1595 with TNFR1 hemizygosity revealed a few genes of interest [Figure 5]. Interestingly, while both drug treatments had overall similar disease suppression effects, a few genes showed differential regulation between the global blockade of infliximab vs the TNFR1-selective drug XPro1595. Thus, Abcb1a [a transmembrane drug transporter], Ccrl1 [an atypical chemokine receptor], Il18r1 and beta defensin 1 [Defb1] were upregulated in TNFdARE/R1het and Xpro1595-treated

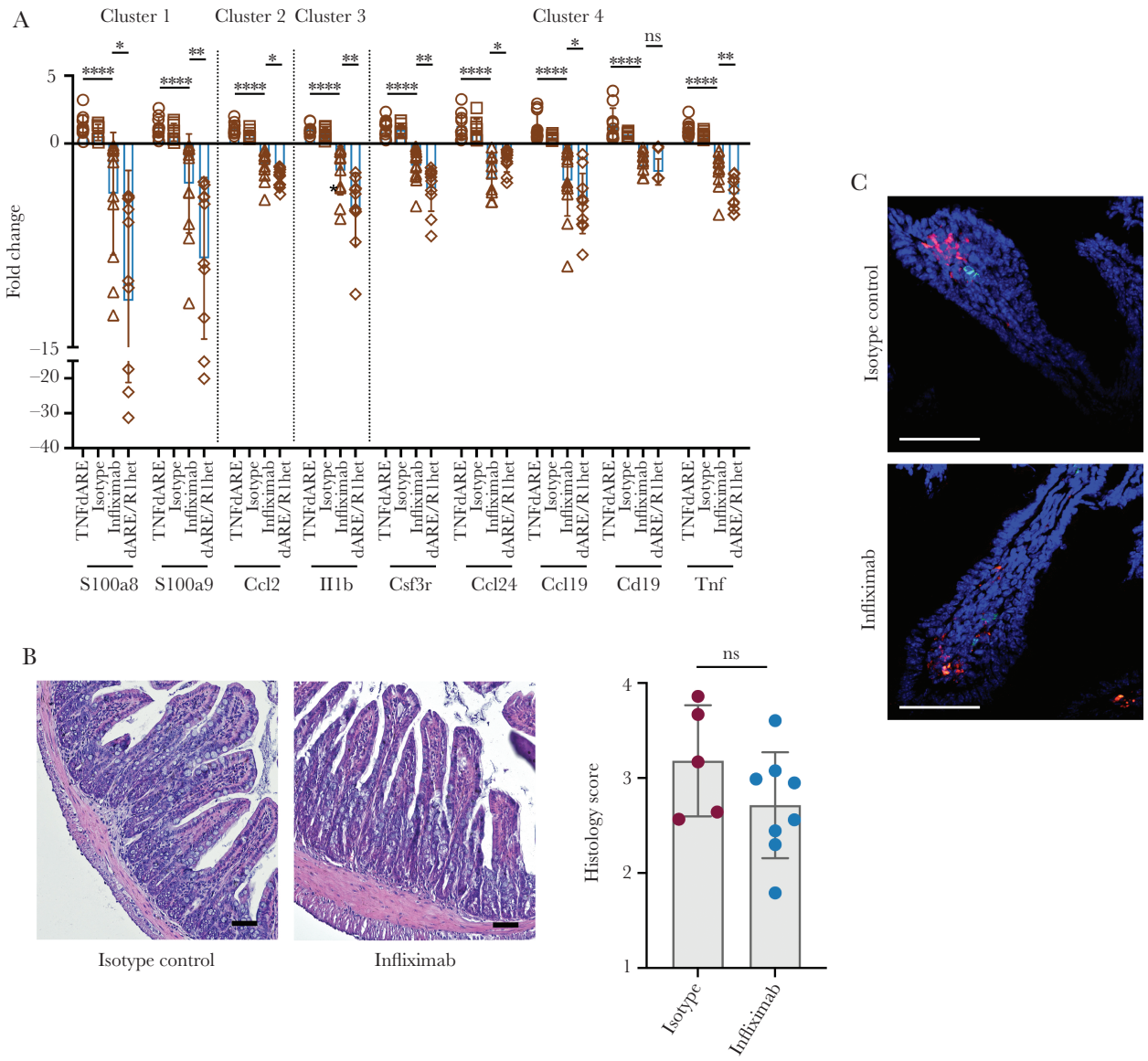

Figure 4. Infliximab administration alleviates ileitis in TNFdARE mice. [A] Pairwise comparison of relative expression of gene clusters. Transcriptional expression was normalized to that of treatment-naive TNFdARE mice and compared between TNFdARE/R1het and TNFdARE mice treated with either an isotype control or infliximab; n = 8–12 mice per group. [B] Representative H&E-stained images from ileal tissue sections of isotype control and infliximab-treated TNFdARE mice [left] along with histology scores [right] [n = 5–8 mice per group]. Scale bar = 50 μm. [C] αB220 [Alexa 488] staining on ileal cryosections from PGRP-S-dsRed+ TNFdARE mice treated with either isotype control [left] or infliximab [right] showing accumulation of B cells [green] and neutrophils [dsRed+] in the villi. Nuclei stained with DAPI. Scale bar = 50 μm [n = 3–4 mice per group]. ns, not significant; *, $p < 0.05$; **, $p < 0.01$; ****, $p < 0.0001$ calculated by non-parametric Mann–Whitney U-test.

mice, but downregulated in infliximab-treated mice. By contrast, Nfatc3 [a T cell transcription factor] was upregulated in TNFdARE/R1het but downregulated by XPro1595 and infliximab. Trem2 [a myeloid cell triggering receptor] was downregulated in both TNFdARE/R1het and Xpro-treated mice, but upregulated by infliximab. Thus, if the protective or homeostatic effect of TNFR1 hemizygosity is mimicked, in part, by the selective targeting effect of XPro1595, these genes, or genes showing similar patterns of regulation, may be connected to this effect.

3.6. Beneficial effect in TNFdARE/R1het mice is associated with enhanced mucosal barrier function

We hypothesized that if there are factors contributing to the stable beneficial effect in TNFdARE/R1het mice, they may be found among genes specifically upregulated in the older TNFdARE/R1het compared to TNFdARE mice. Accordingly, we compared the transcriptional profiles of 10- and 16-week-old TNFdARE/R1het mice with TNFdARE mice and found significant upregulation in the expression of Il-18r and defensin beta 1, with further increases in expression in older mice [Figure 6A]. Importantly, these genes possess immunomodulatory functions and are known to mediate anti-inflammatory responses in the context of microbial infection, chronic inflammation including colitis and maintenance of mucosal barrier functions at the steady state[29–31]. Additionally, histological analysis in TNFdARE mice harbouring an occludin-EGFP fusion reporter transgene revealed discontinuous distribution of occludin throughout the villi, with complete loss of occludin in some areas, associated

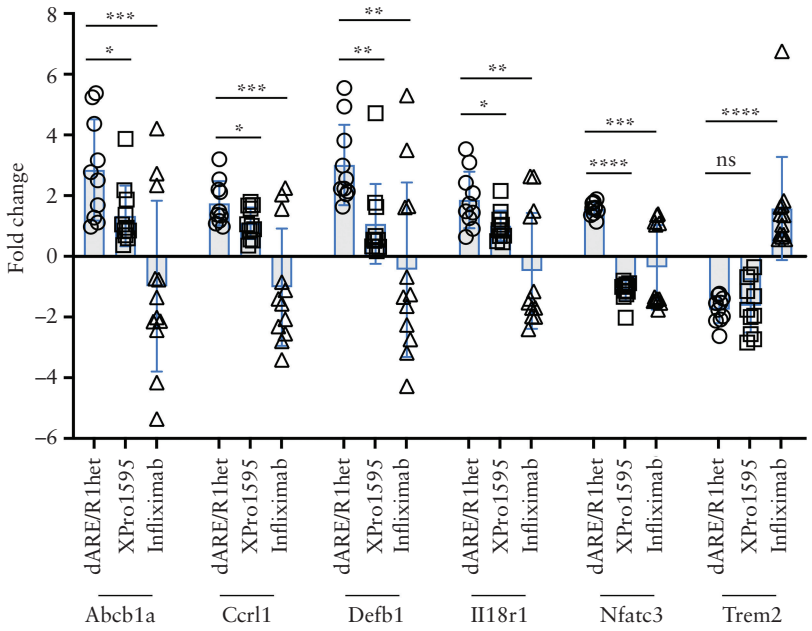

Figure 5. TNFdARE/R1het mice exhibit robust protection from ileitis compared to TNFdARE mice treated with anti-TNF/anti-TNFR1 therapeutic drugs. Pairwise comparison of relative expression of selected genes between TNFdARE/R1het mice [normalized to treatment-naïve TNFdARE mice], XPro1595-treated mice [normalized to BSA-treated controls] and infliximab-treated mice [normalized to isotype control] at the 10-week timepoint [used as an endpoint in drug intervention]; n = 10–12 mice per group. *, $p < 0.05$; **, $p < 0.01$; ***, $p < 0.001$; ****, $p < 0.0001$ calculated by Student's t-test with Welch's correction.

with increased infiltration of inflammatory cells in those villi [Figure 6B]. Importantly, occludin expression was restored in the TNFdARE/R1het mice almost to the levels observed in WT mice that, at least in part, may be linked to the protective benefits in these mice.

3.7. Protective benefit in TNFdARE/R1het mice is associated with decreased inflammatory cell recruitment in the small intestine

To determine whether protection from ileitis in TNFdARE/R1het mice could be mediated by alteration in immune cell recruitment in the villi, we performed flow cytometry to quantitatively measure accumulation of immune cells in the small intestinal lamina propria. In Figure 7, we compare the percentages of lymphocytes [CD3ε^{+}SSC^{lo} T cells and CD19^{+}SSC^{lo} B cells], monocytes [CD11b^{hi}F4/80^{lo}], neutrophils [CD11b^{hi}Ly6G^{hi}] and macrophages [CD11b^{+}F4/80^{+}] between TNFdARE and TNFdARE/R1het mice. There was a significant reduction in the percentages of both monocytes and neutrophils in the TNFdARE/R1het mice in comparison with TNFdARE mice while no significant differences were observed in macrophage and lymphocyte populations. The gating strategy to identify various immune cell populations is shown in Supplementary Figure 4. Collectively, these results indicate that decreased recruitment of inflammatory monocytes and neutrophils in the small intestinal lamina propria of TNFdARE/R1het mice may be directly or indirectly regulated by TNFR1 hemizygosity, thereby contributing to stable long-term protection from progressive ileitis.

4. Discussion

Anti-TNF therapeutics have been used as the major paradigm of treatment in CD, but 'deep remission' encompassing clinical, endoscopic, biomarker and histological remission may be challenging to achieve[32–35]. Despite long-lasting clinical benefits, up to 30–0% of CD patients show clinical and histological non-response to anti-TNF therapy requiring dose change or alternative therapy[36–38]. Interestingly, the studies reported here also highlight that treatment can promote a significant reduction in inflammatory gene expression while showing far less impressive impact on histological markers of disease. Thus, it is important to develop broadly effective therapeutic approaches and perhaps even personalized treatment modalities for patients with CD. We have shown here that TNFR1 hemizygosity in genetically engineered TNFdARE mice provides persistent protection from Crohn's ileitis with benefits more potent compared to that of the anti-TNF biologics tested in this study. However, histological benefits were not observed in TNFdARE/R1het mice despite persistent suppression in inflammatory gene expression, indicating that low-grade inflammation may persist in tissues even when levels of TNFα are significantly reduced [Figure 2A–C]. Overall, our findings demonstrate a crucial role of TNFR1 signalling in the pathogenesis of Crohn's ileitis, suggesting potential benefits from selective targeting of this receptor in developing better therapeutic strategies.

A delicate balance prevails between inflammatory and regulatory pathways through evolution that is essential to maintain immunological tolerance at the intestinal mucosal surface. Dysregulated microbial or immune signals may skew this balance towards inflammation, surpassing the underlying immunoregulatory processes. The phenotypic changes observed in TNFdARE mice provide a close depiction of this situation where prolonged exposure to a highly proinflammatory signal, TNFα, resulted in chronic intestinal inflammation and progressive ileitis.[16] If TNFR1 signalling is the primary mediator of disease, then we can hypothesize that modulation of TNFR1 will produce beneficial effects even in the presence of an inflammatory milieu with chronic TNFα expression. Our

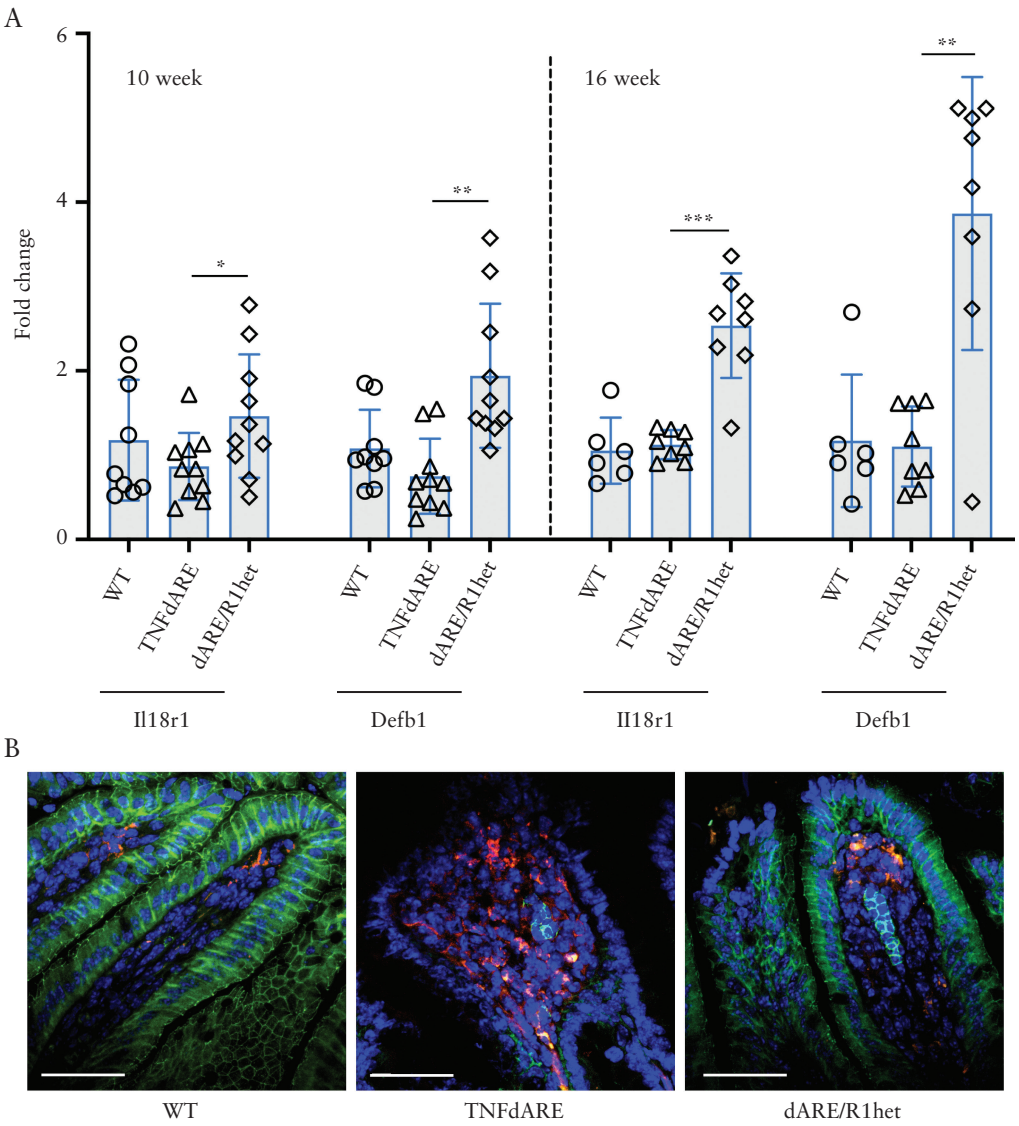

Figure 6. Upregulation of mucosal barrier function in TNFdARE/R1het mice. [A] Comparison between 10- and 16-week-old WT, TNFdARE and TNFdARE/R1het mice based on relative expression of Il18r1 and Defb1. Transcriptional expression was normalized to that in WT littermates; n = 6–10 mice per group. [B] Representative immunofluorescence images showing B cell staining [with αB220-Alexa488 antibody] in distal ileal cryosections obtained from 10-week-old PGRP-S-dsRed+ WT, TNFdARE and TNFdARE/R1het mice [all containing the occludin-eGFP fusion reporter transgene]. Accumulation of B cells and neutrophils in the lamina propria is shown in green and red [dsRed+] respectively. Occludin distribution in the epithelium was determined by green fluorescence originating from occludin-eGFP fusion reporter; n = 3 mice per group. Nuclei stained with DAPI. Scale bar = 50 µm. *, $p < 0.05$; **, $p < 0.01$; ***, $p < 0.001$ calculated by Student's t-test with Welch's correction.

findings with TNFdARE/R1het mice support this hypothesis, indicating that modulation of signalling downstream of TNFR1 may shift the balance towards immune regulation and suppression of disease rather than progression of severe inflammation. In line with this argument, we noted suppression of ileitis in 8-week-old TNFdARE/R1het mice with a more pronounced effect in older mice, suggesting a persistent dominant effect of homeostatic, immune-regulatory mechanisms, which were significantly upregulated in the 16-week-old mice. Importantly, a simultaneous downregulation in Tnfα expression was observed in TNFdARE/R1het mice [Figure 2A–C], which was associated with long-term relative protection from disease, indicating a crucial role of TNFR1 hemizygosity on the transcriptional regulation of TNFα at least in the distal ileum.

Notably, transcriptional expression of Il18r1 and Defb1 was upregulated in the older TNFdARE/R1het mice in comparison with TNFdARE mice. Defensin beta1 is an antimicrobial peptide that is constitutively expressed by all epithelial surfaces including the intestinal epithelium. Its bactericidal properties help mitigate epithelial transmigration of bacterial pathogens, thus contributing to the fortification of innate barrier defences in the gut.[39] Il18r1, on the other hand, is expressed on CD4+ T cells including Foxp3+ Tregs in the intestinal lamina propria, and previous studies have shown that Il18-Il18r1 signalling is crucial in Treg-mediated suppression of inflammation in models of T-cell-transfer-induced colitis.[30] Genetic polymorphisms of human Defb1 and Il18r1 have been implicated in CD and adult- and early-onset inflammatory bowel disease respectively,[40–43] but their direct contribution in disease pathogenesis is not clearly defined. Although the exact nature of these homeostatic pathways needs to be further explored, it can be speculated that attenuation of TNFR1-mediated signalling in TNFdARE/R1het mice

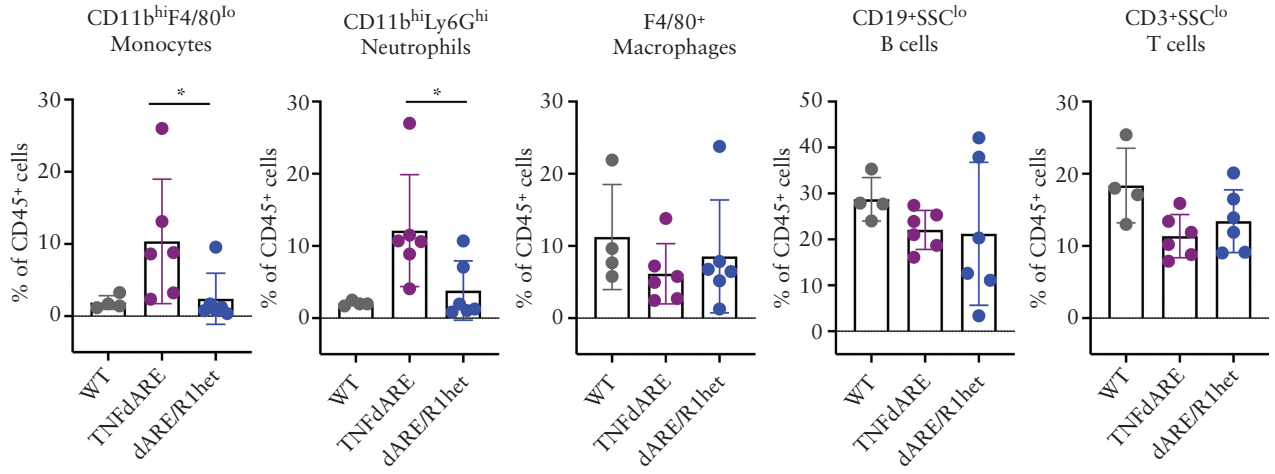

Figure 7. Quantitative analysis of immune cell populations in the small intestinal lamina propria of TNFdARE and TNFdARE/R1het mice. Frequency of immune cell populations in 10- to 12-week-old WT, TNFdARE and TNFdARE/R1het mice determined by flow cytometry. T cells and B cells were defined as CD3ε+SSC^{lo} and CD19+SSC^{lo} respectively, neutrophils were CD11b^{hi}Ly6G^{hi}, monocytes were CD11b^{hi}F4/80^{lo} and macrophages were defined as CD11b^{+}F4/80^{+}; n = 4–6 mice per group. *, $p < 0.05$ calculated by non-parametric Mann–Whitney U-test.

contributes to disease suppression, at least in part by directly or indirectly regulating the expression of the above-mentioned and potentially other intestinal barrier-associated genes.

Surprisingly, the magnitude of disease suppression was more robust in TNFdARE/R1het mice compared to that in TNFdARE mice treated with either XPro1595 or infliximab, suggesting involvement of different molecular mechanisms or regulatory pathways in these differential beneficial effects. One potential contributor to these effects is TNFR2; while infliximab would provide global blockade affecting both TNFR1 and TNFR2 signalling, the TNFR1-selective effect of XPro1595 and TNFR1 hemizygosity will leave TNFR2 signalling intact. Its protective effect in other settings[44–46] may play a role here as well.

Although no clear histological difference was observed between TNFdARE and TNFdARE/R1het mice, flow cytometry analysis with cells isolated from the small intestinal lamina propria provided an interesting scenario. A significant reduction in the recruitment of both monocytes [CD11b^{hi}F4/80^{lo}] and neutrophils [CD11b^{hi}Ly6G^{hi}] was observed in the small intestinal lamina propria of TNFdARE/R1het mice in comparison to TNFdARE mice. In our gene expression analysis, to characterize progression of ileitis in TNFdARE mice, we observed an early induction of Ccl2 expression, which is also a crucial chemoattractant for monocytes in inflamed tissues.[47,48] Moreover, Il1b expression was also stably upregulated in young as well as old TNFdARE mice and has been reported previously in patients with active IBD^{-}.[3,49–51] Studies in murine models of DSS-induced colitis showed that proportions of Il1b-expressing monocytes were significantly elevated in the colonic lamina propria compared to other myeloid cells.[52] In light of this evidence, we propose that early recruitment of monocytes into the mucosa of young TNFdARE mice may be triggered by local elevated levels of Ccl2 that may serve as the initial stimulus promoting progression of ileitis in these mice. This process may be aided by neutrophil recruitment in the tissues, which then contributes to severe inflammation and exacerbation of disease. Although the source and precise role of Il1b in TNFdARE model need to be established, it may be fair to hypothesize that activation of recruited monocytes in the lamina propria contributes to Il1b production and subsequent intestinal inflammation. Consequently, significant downregulation in the transcriptional expression of both Ccl2 and Il1b may constitute immune regulatory or suppressive pathways mediating reduced monocyte recruitment and activation, thereby contributing to disease suppression in TNFdARE/R1het mice.

Supplementary Data

Supplementary data are available online at *ECCO-JCC* online.

Funding

This work was supported by funding from Pfizer Inc. awarded to D.D.L.

Conflict of Interest

The authors disclose no financial conflicts.

Acknowledgments

The authors thank the staff at UCR vivarium for their assistance in mouse care, and Mary Hamer and Vinicius Canale for helpful discussions regarding flow cytometry and histology respectively. The authors also thank Dr Fabio Cominelli [Case Western Reserve University, Cleveland, Ohio] for kindly providing TNFdARE mice, Dr Jerrold R. Turner [Brigham and Women's Hospital and Harvard Medical School] for generously providing villin-eGFP-occludin mice, Pfizer Inc. for providing infliximab and INmune Bio Inc. for providing XPro1595.

Author Contributions

R.C. performed experiments, analysed the data, assembled figures and drafted the manuscript; D.D.L. and R.C. conceptualized and designed the study plan and edited the manuscript; M.R.M. performed principal component analysis on gene expression datasets; R.C., P.T. and D.D.C. performed histology

on tissue sections; R.C., D.D.C., N.M. and M.A. contributed to histopathological scoring. The authors have seen and approved the manuscript.

Data Availability

The normalized gene expression data used as the basis of this study have been posted on an open access public site, Dryad: doi:10.5061/dryad.8cz8w9gr4.

References

1. Neurath MF. Current and emerging therapeutic targets for IBD. *Nat Rev Gastroenterol Hepatol* 2017;14:269–78.
2. Baumgart DC, Sandborn WJ. Crohn's disease. *Lancet* 2012;380:1590–605.
3. Neurath MF. Cytokines in inflammatory bowel disease. *Nat Rev Immunol* 2014;14:329–42.
4. Basson A, Trotter A, Rodriguez-Palacios A, Cominelli F. Mucosal interactions between genetics, diet, and microbiome in inflammatory bowel disease. *Front Immunol* 2016;7:290.
5. Basson AR, Lam M, Cominelli F. Complementary and alternative medicine strategies for therapeutic gut microbiota modulation in inflammatory bowel disease and their next-generation approaches. *Gastroenterol Clin North Am* 2017;46:689–729.
6. Murch SH, Braegger CP, Walker-Smith JA, MacDonald TT. Location of tumour necrosis factor alpha by immunohistochemistry in chronic inflammatory bowel disease. *Gut* 1993;34:1705–9.
7. Van Assche G, Rutgeerts P. Anti-TNF agents in Crohn's disease. *Expert Opin Investig Drugs* 2000;9:103–11.
8. Bradley JR. TNF-mediated inflammatory disease. *J Pathol* 2008;214:149–60.
9. Sedger LM, McDermott MF. TNF and TNF-receptors: from mediators of cell death and inflammation to therapeutic giants – past, present and future. *Cytokine Growth Factor Rev* 2014;25:453–72.
10. Wajant H, Pfizenmaier K, Scheurich P. Tumor necrosis factor signaling. *Cell Death Differ* 2003;10:45–65.
11. Grell M, Douni E, Wajant H, *et al*. The transmembrane form of tumor necrosis factor is the prime activating ligand of the 80 kDa tumor necrosis factor receptor. *Cell* 1995;83:793–802.
12. Ortí-Casañ N, Wu Y, Naudé PJW, De Deyn PP, Zuhorn IS, Eisel ULM. Targeting TNFR2 as a novel therapeutic strategy for Alzheimer's disease. *Front Neurosci* 2019;13:49.
13. Kollias G, Kontoyiannis D. Role of TNF/TNFR in autoimmunity: specific TNF receptor blockade may be advantageous to anti-TNF treatments. *Cytokine Growth Factor Rev* 2002;13:315–21.
14. Tsakiri N, Papadopoulos D, Denis MC, Mitsikostas DD, Kollias G. TNFR2 on non-haematopoietic cells is required for Foxp3+ Treg-cell function and disease suppression in EAE. *Eur J Immunol* 2012;42:403–12.
15. Adegbola SO, Sahnan K, Warusavitarne J, *et al*. Anti-TNF therapy in Crohn's disease. *Int J Mol Sci* 2018;19:2244.
16. Kontoyiannis D, Pasparakis M, Pizarro TT, Cominelli F, Kollias G. Impaired on/off regulation of TNF biosynthesis in mice lacking TNF AU-rich elements: implications for joint and gut-associated immunopathologies. *Immunity* 1999;10:387–98.
17. Wang J, Gusti V, Saraswati A, Lo DD. Convergent and divergent development among M cell lineages in mouse mucosal epithelium. *J Immunol* 2011;187:5277–85.
18. Marchiando AM, Shen L, Graham WV, *et al*. Caveolin-1-dependent occludin endocytosis is required for TNF-induced tight junction regulation in vivo. *J Cell Biol* 2010;189:111–26.
19. Pielou EC. *The Interpretation of Ecological Data: A Primer on Classification and Ordination*. John Wiley & Sons; 1984.
20. Kontoyiannis D, Boulougouris G, Manoloukos M, *et al*. Genetic dissection of the cellular pathways and signaling mechanisms in modeled tumor necrosis factor-induced Crohn's-like inflammatory bowel disease. *J Exp Med* 2002;196:1563–74.
21. Steed PM, Tansey MG, Zalevsky J, *et al*. Inactivation of TNF signaling by rationally designed dominant-negative TNF variants. *Science* 2003;301:1895–8.
22. McCoy MK, Martinez TN, Ruhn KA, *et al*. Blocking soluble tumor necrosis factor signaling with dominant-negative tumor necrosis factor inhibitor attenuates loss of dopaminergic neurons in models of Parkinson's disease. *J Neurosci* 2006;26:9365–75.
23. Brambilla R, Ashbaugh JJ, Magliozzi R, *et al*. Inhibition of soluble tumour necrosis factor is therapeutic in experimental autoimmune encephalomyelitis and promotes axon preservation and remyelination. *Brain* 2011;134:2736–54.
24. Barnum CJ, Chen X, Chung J, *et al*. Peripheral administration of the selective inhibitor of soluble tumor necrosis factor (TNF) XPro®1595 attenuates nigral cell loss and glial activation in 6-OHDA hemiparkinsonian rats. *J Parkinsons Dis* 2014;4:349–60.
25. Akobeng AK, Zachos M. Tumor necrosis factor-alpha antibody for induction of remission in Crohn's disease. *Cochrane Database Syst Rev* 2004:CD003574.
26. Ljung T, Karlén P, Schmidt D, *et al*. Infliximab in inflammatory bowel disease: clinical outcome in a population based cohort from Stockholm County. *Gut* 2004;53:849–53.
27. Present DH, Rutgeerts P, Targan S, *et al*. Infliximab for the treatment of fistulas in patients with Crohn's disease. *N Engl J Med* 1999;340:1398–405.
28. Targan SR, Hanauer SB, van Deventer SJ, *et al*. A short-term study of chimeric monoclonal antibody cA2 to tumor necrosis factor alpha for Crohn's disease. Crohn's Disease cA2 Study Group. *N Engl J Med* 1997;337:1029–35.
29. Nowarski R, Jackson R, Gagliani N, *et al*. Epithelial IL-18 equilibrium controls barrier function in colitis. *Cell* 2015;163:1444–56.
30. Harrison OJ, Srinivasan N, Pott J, *et al*. Epithelial-derived IL-18 regulates Th17 cell differentiation and Foxp3$^+$ Treg cell function in the intestine. *Mucosal Immunol* 2015;8:1226–36.
31. Morrison G, Kilanowski F, Davidson D, Dorin J. Characterization of the mouse beta defensin 1, Defb1, mutant mouse model. *Infect Immun* 2002;70:3053–60.
32. Colombel JF, Rutgeerts PJ, Sandborn WJ, *et al*. Adalimumab induces deep remission in patients with Crohn's disease. *Clin Gastroenterol Hepatol* 2014;12:414–22.e5.
33. Zallot C, Peyrin-Biroulet L. Deep remission in inflammatory bowel disease: looking beyond symptoms. *Curr Gastroenterol Rep* 2013;15:315.
34. Molander P, Sipponen T, Kemppainen H, *et al*. Achievement of deep remission during scheduled maintenance therapy with TNFα-blocking agents in IBD. *J Crohns Colitis* 2013;7:730–5.
35. Hazel K, O'Connor A. Emerging treatments for inflammatory bowel disease. *Ther Adv Chronic Dis* 2020;11:2040622319899297.
36. Sandborn WJ, Rutgeerts P, Enns R, *et al*. Adalimumab induction therapy for Crohn disease previously treated with infliximab: a randomized trial. *Ann Intern Med* 2007;146:829–38.
37. Sandborn WJ, Abreu MT, D'Haens G, *et al*. Certolizumab pegol in patients with moderate to severe Crohn's disease and secondary failure to infliximab. *Clin Gastroenterol Hepatol* 2010;8:688–95. e2.
38. Yarur AJ, Rubin DT. Therapeutic drug monitoring of anti-tumor necrosis factor agents in patients with inflammatory bowel diseases. *Inflamm Bowel Dis* 2015;21:1709–18.
39. Raschig J, Mailänder-Sánchez D, Berscheid A, *et al*. Ubiquitously expressed Human Beta Defensin 1 (hBD1) forms bacteria-entrapping nets in a redox dependent mode of action. *PLoS Pathog* 2017;13:e1006261.
40. Kocsis AK, Lakatos PL, Somogyvári F, *et al*. Association of beta-defensin 1 single nucleotide polymorphisms with Crohn's disease. *Scand J Gastroenterol* 2008;43:299–307.
41. Barrett JC, Hansoul S, Nicolae DL, *et al*.; NIDDK IBD Genetics Consortium; Belgian-French IBD Consortium; Wellcome Trust Case Control Consortium. Genome-wide association defines more than 30 distinct susceptibility loci for Crohn's disease. *Nat Genet* 2008;40:955–62.

42. Imielinski M, Baldassano RN, Griffiths A, *et al*.; Western Regional Alliance for Pediatric IBD; International IBD Genetics Consortium; NIDDK IBD Genetics Consortium; Belgian-French IBD Consortium; Wellcome Trust Case Control Consortium. Common variants at five new loci associated with early-onset inflammatory bowel disease. *Nat Genet* 2009;41:1335–40.
43. Hedl M, Zheng S, Abraham C. The IL18RAP region disease polymorphism decreases IL-18RAP/IL-18R1/IL-1R1 expression and signaling through innate receptor-initiated pathways. *J Immunol* 2014;192:5924–32.
44. Punit S, Dubé PE, Liu CY, Girish N, Washington MK, Polk DB. Tumor necrosis factor receptor 2 restricts the pathogenicity of CD8(+) T cells in mice with colitis. *Gastroenterology* 2015;149:993–1005.e2.
45. Chen X, Wu X, Zhou Q, Howard OM, Netea MG, Oppenheim JJ. TNFR2 is critical for the stabilization of the CD4+Foxp3+ regulatory T. cell phenotype in the inflammatory environment. *J Immunol* 2013;190:1076–84.
46. Yang S, Xie C, Chen Y, *et al*. Differential roles of TNFα-TNFR1 and TNFα-TNFR2 in the differentiation and function of CD4+Foxp3+ induced Treg cells in vitro and in vivo periphery in autoimmune diseases. *Cell Death Dis* 2019;10:27.
47. Platt AM, Bain CC, Bordon Y, Sester DP, Mowat AM. An independent subset of TLR expressing CCR2-dependent macrophages promotes colonic inflammation. *J Immunol* 2010;184:6843–54.
48. Zigmond E, Varol C, Farache J, *et al*. Ly6C hi monocytes in the inflamed colon give rise to proinflammatory effector cells and migratory antigen-presenting cells. *Immunity* 2012;37:1076–90.
49. Cappello M, Keshav S, Prince C, Jewell DP, Gordon S. Detection of mRNAs for macrophage products in inflammatory bowel disease by in situ hybridisation. *Gut* 1992;33:1214–9.
50. Hart AL, Al-Hassi HO, Rigby RJ, *et al*. Characteristics of intestinal dendritic cells in inflammatory bowel diseases. *Gastroenterology* 2005;129:50–65.
51. Middel P, Raddatz D, Gunawan B, Haller F, Radzun HJ. Increased number of mature dendritic cells in Crohn's disease: evidence for a chemokine mediated retention mechanism. *Gut* 2006;55:220–7.
52. Jones GR, Bain CC, Fenton TM, *et al*. Dynamics of colon monocyte and macrophage activation during colitis. *Front Immunol* 2018;9:2764.